Ultrasound in Med. & Biol., Vol. 32, No. 6, pp. 905–914, 2006

0301-5629/06/$–see front matter

ELSEVIER

doi:10.1016/j.ultrasmedbio.2006.03.004

● *Original Contribution*

# TRANSFECTION EFFECT OF MICROBUBBLES ON CELLS IN SUPERPOSED ULTRASOUND WAVES AND BEHAVIOR OF CAVITATION BUBBLE

TETSUYA KODAMA,*† YUKIO TOMITA,‡ KEN-ICHIRO KOSHIYAMA,§ and MARTIN J.K. BLOMLEY*

*Imaging Sciences Department, Clinical Sciences Division, Faculty of Medicine, Imperial College London, Hammersmith Campus, London , UK; †Biomedical Engineering Research Organization, Tohoku University, Sendai, Japan; ‡Faculty of Education, Hokkaido University of Education, Hakodate, Japan; and §Graduate School of Engineering, Hokkaido University, Sapporo, Japan

(*Received* 4 *October* 2005; *revised* 27 *February* 2006; *in final form* 7 *March* 2006)

**Abstract—The combination of ultrasound and ultrasound contrast agents (UCAs) is able to induce transient membrane permeability leading to direct delivery of exogenous molecules into cells. Cavitation bubbles are believed to be involved in the membrane permeability; however, the detailed mechanism is still unknown. In the present study, the effects of ultrasound and the UCAs, Optison™ on transfection *in vitro* for different medium heights and the related dynamic behaviors of cavitation bubbles were investigated. Cultured CHO-E cells mixed with reporter genes (luciferase or β-gal plasmid DNA) and UCAs were exposed to 1MHz ultrasound in 24-well plates. Ultrasound was applied from the bottom of the well and reflected at the free surface of the medium, resulting in the superposition of ultrasound waves within the well. Cells cultured on the bottom of 24-well plates were located near the first node (displacement node) of the incident ultrasound downstream. Transfection activity was a function determined with the height of the medium (wave traveling distance), as well as the concentration of UCAs and the exposure time was also determined with the concentration of UCAs and the exposure duration. Survival fraction was determined by MTT assay, also changes with these values in the reverse pattern compared with luciferase activity. With shallow medium height, high transfection efficacy and high survival fraction were obtained at a low concentration of UCAs. In addition, capillary waves and subsequent atomized particles became significant as the medium height decreased. These phenomena suggested cavitation bubbles were being generated in the medium. To determine the effect of UCAs on bubble generation, we repeated the experiments using crushed heat-treated Optison™ solution instead of the standard microbubble preparation. The transfection ratio and survival fraction showed no additional benefit when ultrasound was used. These results suggested that cavitation bubbles created by the collapse of UCAs were a key factor for transfection, and their intensities were enhanced by the interaction of the superpose ultrasound with the decreasing the height of the medium. Hypothesizing that free cavitation bubbles were generated from cavitation nuclei created by fragmented UCA shells, we carried out numerical analysis of a free spherical bubble motion in the field of ultrasound. Analyzing the interaction of the shock wave generated by a cavitation bubble and a cell membrane, we estimated the shock wave propagation distance that would induce cell membrane damage from the center of the cavitation bubble.**
**(E-mail: kodama@tubero.tohoku.ac.jp)** 

*Key Words:* **Molecular delivery, Cavitation bubbles, CHO-E cells, Membrane permeabilization.**

## INTRODUCTION

The plasma membrane is a thin film (approximately 5 nm) of lipid and protein molecules held together mainly by noncovalent interactions. The lipid bilayer provides a basic structure of the membrane and the protein molecules exist as dissolved entities in this layer. This thin layer encloses the cell, defines its boundary and the protein embedded therein performs a multitude of functions, such as the regulation of ion gradients across membranes and ATP synthesis (Lee 2004). In molecular delivery, it is desired to deliver macromolecules and small polar molecules across the membranes. However, in most cases, this thin layer serves as a relatively im-

Address correspondence to: Tetsuya Kodama, Ph.D., Biomedical Engineering Research Organization, Tohoku University, 2-1 Seiryo-machi, Aoba-ku, Sendai 980-8575, Japan. E-mail: kodama@tubero.tohoku.ac.jp

permeable barrier to the passage of these molecules (Dokka and Rojanasakul 2000).

The combination of ultrasound contrast agents (UCAs) and ultrasound has been shown to induce transient membrane permeability leading to direct delivery of exogenous molecules into cells. This method is nontoxic and nonimmunogenic, and has been applied for both *in vitro* and *in vivo* experimental gene therapy studies with varying degrees of success (Bekeredjian et al. 2003; Danialou et al. 2002; Kodama et al. 2005; Lu et al. 2003; Taniyama et al. 2002; Wang et al. 2005; Zarnitsyn and Prausnitz 2004). Recently, review papers have been published in both areas (Koike et al. 2005; Lindner 2004; Mehier-Humbert and Guy 2005; Yang et al. 2005). Although this method has significant advantages compared with other chemical and virus methods, efficacy of molecular delivery is relatively low, and the mechanism of molecular transfer, as well as the methodology, has not been elucidated or optimized.

Many studies have used mainly two different delivery methods. One is to expose ultrasound to suspended cells (Bao et al. 1997; Brayman and Miller 1997; Everbach et al. 1997; Feril et al. 2003; Kamaev et al. 2004; Li et al. 2003; Zarnitsyn and Prausnitz 2004). Another is to expose ultrasound to adherent cells from either the top of medium (Lawrie et al. 2000) or the bottom of culture plates (Chen et al. 2004; Greenleaf et al. 1998). The cell suspension system has several advantages over the transfection of adherent cells, *i.e.*, routine passage, higher cell densities, easer product titers and scalable methodology.

However, when adherent cells are suspended, adhesion-generated signals would affect the regulation of signaling pathways, resulting in different cellular response (Aplin et al. 2002; Carstens et al. 1996). Therefore, adherent cells are preferable to be transfected in adhesion. Furthermore, since adherent cells are easier to transfect than suspension cells (Cheng et al. 2004), the methodology of transfection using ultrasound and UCAs would be improved and optimized using adherent cells.

As ultrasound is generated at a fixed position, standing waves are generated. Pickworth et al. (Pickworth et al. 1989) generated standing waves without acoustic absorbers in a water tank, and exposed the waves to cells located either at nodes or at antinodes of displacement. It was found that viability of cells would be different at each position (Pickworth et al. 1989). This would appear to indicate that fluid motion is involved in cell membrane damage and the subsequent molecular delivery.

In the present study, we investigated the effect of superposed ultrasound and the UCA, Optison™, on transfection of CHO-E cells located at a node of displacement. Ultrasound was introduced from the bottom of the well and reflected at the free surface of the transfection medium, resulting in superposed ultrasound in the well. The intensity of superposed ultrasound was controlled by changing the height of medium and the incident ultrasound.

From the observations of cavitation bubble generation, the subsequent dynamics of cavitation bubbles was analyzed.

## METHODS

### *Cell preparation*

Chinese hamster ovary (CHO) cells expressing human E-selectin (CHO-E) from Professor D. O. Haskard (Imperial College, London, UK) were maintained in F-12 Nutrient Mixture media (Invitrogen, Carlsbad, CA, USA) supplemented with 10% fetal bovine serum, 1% penicillin-streptomycin and 400 $\mu$g/mL Zeocin (Invitrogen). All cells were cultured in 75 $cm^2$ flasks at 37°C in a 5% $CO_2$ incubator. Both total cell counts and the initial cell viability were determined with a hemocytometer, using the trypan blue dye exclusion method (Tennant 1964) before ultrasound-mediated transfection experiments. In all cases, cells were grown to 90% confluence, harvested using trypsin-EDTA and showed 99% viability. After UCA-mediated transfection, the cells were washed once using phosphate-buffered saline without $Ca^{2+}$ and $Mg^{2+}$. One half of the cells was used for the luciferase assay, and the other half was used for the cell viability assay. Cell viability was determined using MTT (3-[4,5-dimethylthiazol-2-yl]-2,5-diphenyltetrazolium bromide) assay as previously described (Kodama et al. 2003), and cell survival fractions expressed relative to control cells not treated with either UCAs or ultrasound.

### *Plasmid*

The luciferase reporter vector pGL3-control (5256 bp), which expresses luciferase from an SV40 promoter, and pCMV$\beta$ vector (7164 bp), which expresses $\beta$-galactosidase from the human cytomegalovirus immediate early gene promoter, were obtained from Promega (Madison, WI, USA) and Clontech (Palo Alto, CA, USA), respectively. The plasmid was propagated in XL1-Blue subcloning-grade competent cells (Stratagene Co., La Jolla, CA, USA), and purified using endotoxin-free plasmid DNA purification kits (QIAGEN Inc., Valencia, CA, USA). The purity of the plasmid preparation was determined by 0.8% agarose gel electrophoresis. DNA concentration was determined by UV absorption at 260 nm using a spectrophotometer (DU640 UV/Visible Spectrophotometer, Beckman, Fullerton, CA, USA). In all cases an $OD_{260/280}$ ratio of 1.71 $\pm$ 0.03 was obtained.

### *Ultrasound*

Ultrasound was generated by a 1-MHz therapeutic ultrasound (duty cycle 20%, with a pulse repetition pe-

riod of 10 ms, 30 mm in diameter, Therasonic Therapy Unit, Electro-Medical Supplies Ltd., Oxfordshire, UK) (Lu et al. 2003). The nominal spatial peak-temporal average (SPTA) intensity varied from 0.5 to 3.0 W/cm$^2$. The pressure values were measured at a stand-off distance of 1 mm from the transducer surface with a PVDF needle-hydrophone (PVDF-Z44-1000, Specialty Engineering Associates, Soquel, CA, USA). The maximum pressure values were measured by the moving distance of the hydrophone along the diameter of the transducer. The signals were recorded into a digital phosphor oscilloscope (TDS7154, Tektronix, Beaverton, OR, USA). There was no difference between pressures with and without the culture plate. Therefore, the attenuation of ultrasound by the plate material was negligible (data not shown).

*Ultrasound contrast agents (UCAs)*

Optison$^{TM}$ contrast agent (Amersham Health, Oslo, Norway) was used. Optison$^{TM}$ consists of octafluoropropane-filled albumin microspheres that have a mean diameter of between 3.0 and 4.5 $\mu$m. The concentration is 5.0 to 8.0 $\times$ 10$^8$ microbubbles/ml (http://www.amershamhealth-us.com/optison/). In this study, the mean concentration was set to the arithmetic average of 6.5 $\times$ 10$^8$ microbubbles/mL and the mean diameter was simply set to 4.0 $\mu$m.

*Crushed heat-treated Optison$^{TM}$*

Optison$^{TM}$ was disrupted in a 1-mL syringe by application of positive and negative pressures by hand, and then heated-treated in water bath at 65°C for 30 min. It was confirmed by an optical microscope (CX31, Olympus, Tokyo, Japan) that there were no residual bubbles below the limits of resolution of the optical microscope (<200 nm).

*Transfection*

CHO-E cells were seeded in 24-well (16-mm in diameter/well) plates alternately at 1 $\times$ 10$^5$ cells/well in complete media at 37°C in a 5% $CO_2$ incubator. After a 24 h attachment period, the seeded cells were washed with PBS, and the medium replaced with fresh media (200 to 3000 $\mu$L), containing pGL3-control (40 $\mu$g/mL) or pCMV$\beta$ (40 $\mu$g/mL) with and without Optison$^{TM}$ (0.1 to 40% vol/vol). The 24-well plates were located just above the ultrasound probe in a test chamber (380 $\times$ 250 $\times$ 130 mm$^3$) filled with water, as shown in Fig. 1, and exposed to ultrasound. Since cells were seeded into wells alternately, neighboring wells were not exposed to ultrasound at the same time. The plates were incubated for 1.5 h at 37°C in a 5% $CO_2$ incubator, supplemented with 300 $\mu$L of complete media, and then incubated for another 24 h at 37°C in a 5% $CO_2$ incubator.

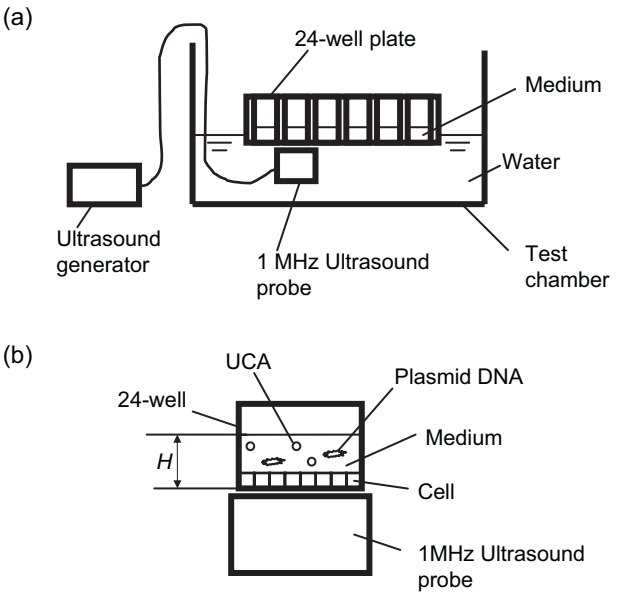


Fig. 1. Experimental setup. (a) A 24-well plate containing CHO-E cells was placed just above a flat 1-MHz ultrasound transducer. Since the thickness of the plate was 1 mm, cells were located near the first node of ultrasound downstream if the sound velocity was 1500 m/s. (b) The setup of transfection. The medium height, *H*, was varied from 1 mm to 15 mm.

*Luciferase assay*

Twenty-four hours after ultrasound treatment, the cells were washed (PBS), lysed with 200 $\mu$L of Reporter Lysis Buffer (Promega), and subsequently frozen at −80°C until required. When required, the cells were defrosted on ice. Each lysate was centrifuged to pellet cell debris at 12,000 *g* for 2 min. Twenty $\mu$L of the lysate was examined for luciferase activity with 100 $\mu$L of luciferase assay reagent containing D-Lucifer (Promega). Luminescence emissions were measured as relative light units (RLU) at 25°C for 10 s using a luminometer (TD-20/20, Turner BioSystems, Inc., Sunnyvale, CA, USA). Total protein content was calculated using albumin standard curves (BCA protein assay kit, Pierce, Rockford, IL, USA). All standards and samples were performed in duplicate. In all cases, mean protein absorbance was measured at 562 nm using a plate reader (SpectraMax, Molecular Device Corp., Sunnyvale, CA). Luciferase activity was converted to RLU/mg protein.

*$\beta$-gal activity*

Twenty-four hours after ultrasound treatment, the transfected cells were washed (with PBS), fixed and then stained to reveal $\beta$-gal activity, as previously described (Dannenberg and Suga 1981). The image of cells was photographed using a digital camera (DP10, Olympus)

Table 1. Ultrasound parameters

| I (W/cm$^2$) | $P_A$ (MPa) | $I_A$ (W/cm$^2$) | $E_A$ (J/cm$^2$) | $T_w$ (mm) | $MI_A$ |
|---|---|---|---|---|---|
| 0.5 | 0.19 | 1.3 | 0.25 | 15 | 0.19 |
| 1.0 | 0.23 | 1.9 | 0.36 | 15 | 0.23 |
| 2.0 | 0.26 | 2.3 | 0.46 | 15 | 0.26 |
| 3.0 | 0.28 | 2.6 | 0.52 | 15 | 0.28 |

The nominal intensity, $I$, varied from 0.5 to 3.0 W/cm$^2$. The duty cycle was 20%. The peak positive pressure, $P_A$, was obtained near the center of the transducer surface. The values of the peak positive pressures were the same as those of the peak negative pressures, $P$-. The width of the peak pressure at −6 dB compression was given as, $T_w$. The acoustic intensity $I_A$ defined as $I_A = P^2_A/2\rho_L C_L$, energy density, $E_A$, given as $I_A \times$ (duty cycle), *i.e.,* $E_A = I_A \times 0.2$. The mechanical index, $MI_A$ was defined as $MI_A = (P_A/\text{MPa})/(f/\text{MHz})^{1/2}$, where $f = 1$ MHz. The ultrasound parameters were measured by a PVDF needle hydrophone at a stand-off distance of 1 mm from the transducer surface. The pressure values varied in the Gaussian distribution along the diameter of 30 mm. $T_w$ was about 15 mm, which was comparable to the diameter (16 mm) of the individual wells for a 24-well plate. Thus, all cells seeded on the bottom of the well would be exposed to ultrasound within the half width of the pressure.

mounted on a stereo microscope (SZX12, Olympus). The number of β-gal positive colonies in mm$^2$ along the diameter of a 24-well was counted ($n = 3$) on a Macintosh (PowerPC G4) computer using the public domain NIH Image program (developed at the U.S. National Institutes of Health and available on the Internet at http://rsb.info.nih.gov/nih-image/).

*Statistical analysis*

All measurements are expressed as mean ± S.E.M. Comparisons between samples were made using two-way factorial ANOVA. Differences were considered to be significant at $p < 0.05$.

## RESULTS

*Evaluation of ultrasound parameters*

To accurately determine the intensity of ultrasound that the cells would be subjected to at the ultrasound superposition, we calibrated our experimental set-up using a PVDF hydrophone following exposure to various intensities near the first node (displacement node) of the incident ultrasound downstream at a distance of 1 mm from the transducer surface (see Fig. 1). Table 1 shows the ultrasound parameters generated by the ultrasound transducer with various parameters. The nominal intensity, $I$, varied from 0.5 to 3.0 W/cm$^2$. The values of peak positive pressures $P_A$ were the same as those of negative pressures. The experimental acoustic intensity, $I_A$ was calculated from $P_A$ (see legend to Table 1). $I_A$ increased linearly with increasing $I$; however, this relationship deviated at the higher intensity where the maximum pressure was 0.28 MPa at $I = 3.0$ W/cm$^2$. The pressure values varied in the Gaussian distribution along the diameter of 30 mm. The width of the positive pressure at −6dB compression, $T_w$, was about 15 mm, which was comparable to the diameter (16 mm) of the individual wells for a 24-well plate. Thus, all cells seeded on the bottom of the well would be exposed to ultrasound within the half width of the pressure. The mechanical index, $MI_A$, was 0.19 to 0.28. When the derating factor of 0.3 dB/cm-MHz, $MI_A$ is considered (Abbott 1999), $MI_A$ is decreased further. This reduced $MI_A$ is less than 0.7 and, thus, it is assumed that ultrasound alone would produce no cavitation bubbles in the media (Fowlkes 2000). For the ultrasound intensity, the experimentally determined intensity $I_A$ was used rather than the nominal intensity $I$, in our experiments.

*Gene transfection and survival fraction by superposed ultrasound and UCAs*

The superposed ultrasound used in our experiments was generated by the interaction of incident ultrasound from the bottom of culture plates and reflected ultrasound at the free surface of the experimental cell culture medium. In all cases, the intensity of the superposed ultrasound was dependent on the initial acoustic intensity and distance of wave propagation between the surface at the bottom of the well and the free surface of the cell culture medium. First, we investigated the effect of the ultrasound alone on cytotoxicity at varying acoustic intensity $I_A$ and exposure time $T_A$, at a cell culture medium depth of $H = 1$ mm. The survival fraction was obtained by MTT assay. Although the survival fraction in all cases was close to unity (Fig. 2), cell cytotoxicity was observed at $I_A = 2.3$ W/cm$^2$ for $T_A = 120$ s ($p < 0.01$) and at $I_A = 2.6$ W/cm$^2$ for $T_A = 60$s ($p < 0.05$) and 120s ($p < 0.01$). Accordingly, intensities of $I_A = 1.3$ W/cm$^2$ and

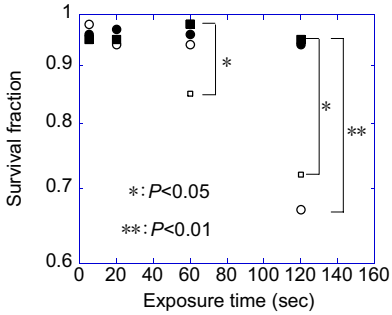


Fig. 2. Survival fractions determined by the MTT assay of CHO-E cells treated with increasing exposure times of ultrasound alone for varying ultrasound intensities. $I_A = 1.3$ W/cm$^2$ (filled circle), $I_A = 1.9$ W/cm$^2$ (filled square), $I_A = 2.3$ W/cm$^2$ (open circle), $I_A = 2.6$ W/cm$^2$ (open square). The initial height of medium was $H = 1.0$ mm. Values are means of 3 to 6 ± S.E.M. of at least three experiments.

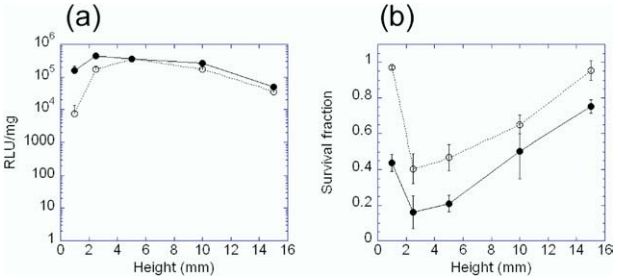


Fig. 3. Effect of the height of medium on luciferase activity and viability of CHO-E cells. (a) Luciferase activity, (b) Survival fractions measured by the MTT assay. Ultrasound and UCAs (filled circle), ultrasound alone (open circle). Acoustic intensity was $I_A$ = 1.9 W/cm$^2$. The exposure time, $T_A$, was 20 s. The UCA concentration was 5% (vol/vol). The concentration of plasmid pGL3-control was 20 $\mu$g/mL.

$I_A$ = 1.9 W/cm$^2$ were used in subsequent transfection experiments.

Next we investigated the effect of the height of the complete medium $H$, *i.e.*, distance of wave propagation, on cell transfection and survival fraction (Fig. 3). The UCAs concentration was 5% (vol/vol) while the acoustic intensity was maintained at $I_A$ = 1.9 W/cm$^2$, and the duration of ultrasound irradiation $T_A$ was 20 s. Ultrasound irradiation at the acoustic pressures used resulted in UCA destruction, demonstrated by the rapid change to transparency of the initially white emulsified medium that contained Optison™. After ultrasound exposure, the medium became transparent within a second, and white flowing debris was observed in the medium. As the height of the medium decreased, the intensity of capillary waves at the medium surface increased, and subsequent atomized liquid particles started to fly from the surface. These adhered to the well cover plates, resulting in formation of water drops. The diameter of the particles was calculated to be 7.9 $\mu$m from eqn (1). The phenomenon was observed down to UCA concentrations of 0.1% (vol/vol). However, atomized particles were rarely observed when no UCAs were added to the media. This rapid UCA collapse, significant instability of the free surface, and resultant atomized particles indicate collateral evidence of the existence of cavitation bubbles in the medium. The tendency of the gene expression was found against the survival fraction for different heights, *i.e.*, as the efficacy of molecular delivery increases, the cytotoxicity increases. Maximum gene expression was 4.4 $\times$ 10$^5$ $\pm$ 8.1 $\times$ 10$^4$ RLU/mg at $H$ = 2.5 mm, where mg of protein is intended as a measure of total number of cells present. On the other hand, the survival fraction reached a minimum value of 0.16 $\pm$ 0.09. From Fig. 3a and b, it is possible that the effect of microbubbles is dominant in the rage of 1 to 2 mm height and is not significant over 2 to 16 mm range.

Next, we investigated the distribution of transfected cells over the well surface at a representative medium heights ($H$ = 1 mm and $H$ = 15 mm). Cells were transfected with $\beta$-gal plasmid DNA for visualization. At medium heights $H$ = 1 mm (Fig. 4a), we noted that most cells were detached from the center of the wells while $\beta$-gal positive colonies were only detected at well fringes. In contrast, $\beta$-gal positive colonies were uniformly distributed over the well surface for $H$ = 15 mm (Fig. 4b). Figure 4c and d show the number of $\beta$-gal positive colonies in mm$^2$ across the well diameter [(= 2 $\times$ $r$, $r$: radius = 8 mm)] of triplicate 24-wells for $H$ = 1 mm (Fig. 4a) and $H$ = 15 mm (Fig. 4b), respectively, where the normalized radius is shown as $r$*. The number of the positive colonies was counted regardless of their size. In this way, the number of counted positive colonies was qualitatively related to the total gene expression per well. Figure 4a shows that there were no positive colonies near the central area for $H$ = 1 mm, and that the number of colonies increased with increasing distance from the center to $r$* = 1 and $r$* = $-$1, where the number of $\beta$-gal positive colonies was 50/mm$^2$. In the case of $H$ = 15 mm (Fig. 4d), the positive colonies were uniformly distributed irrespective of the distance from the center, where the number of $\beta$-gal positive colonies was 31.9 $\pm$ 1.8/ mm$^2$. As shown in Table 1, the energy density showed an approximately Gaussian distribution.

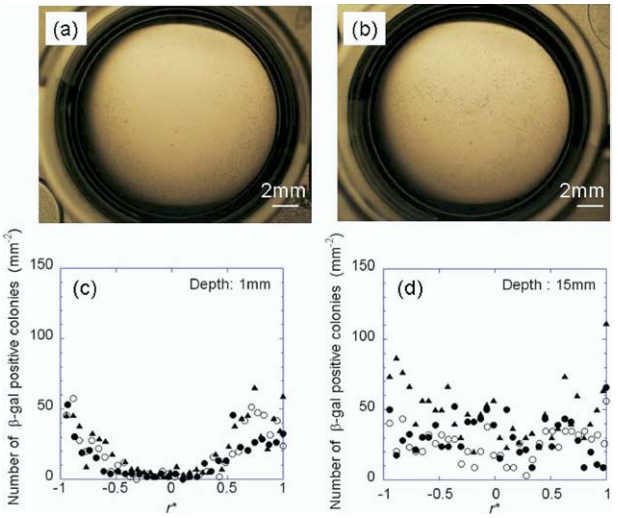


Fig. 4. Distribution of $\beta$-gal positive cells on a 24-well. $H$ = 1 mm (a and c) and $H$ = 15 mm (b and d). Number of $\beta$-gal positive colonies in mm$^2$ along the diameter ( = 2 $\times$ $r$, $r$: radius) of a well of the 24-well plate, where $r$* is normalized radius with $r$. The number of colonies was counted from triplicate wells (open circle, filled circle, filled triangle). The UCA concentration was 5% (vol/vol). The concentration of plasmid pCMV$\beta$ was 20 $\mu$g/mL. The acoustic intensity was $I_A$ = 1.9 W/cm$^2$. The exposure time was $T_A$ = 20 s. The UCA concentration was 5% (vol/vol). Scale bar indicates 2 mm.

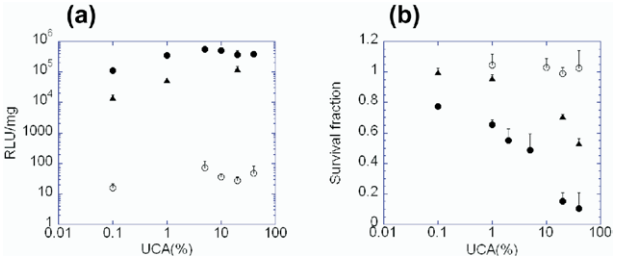


Fig. 5. Effect of the UCA concentrations on the luciferase activity and viability of CHO-E cells at a height of $H = 1$ mm. (a) Luciferase activity, (b) survival fractions measured by the MTT assay. Acoustic intensity was $I_A = 1.3$ W/cm$^2$ (filled triangle) and $I_A = 1.9$ W/cm$^2$ (filled circle). UCAs alone, *i.e.*, $I_A = 0$ W/cm$^2$ (open circle). The exposure time, $T_A$, was 20 s. The concentration of plasmid pGL3-control was 20 $\mu$g/mL.

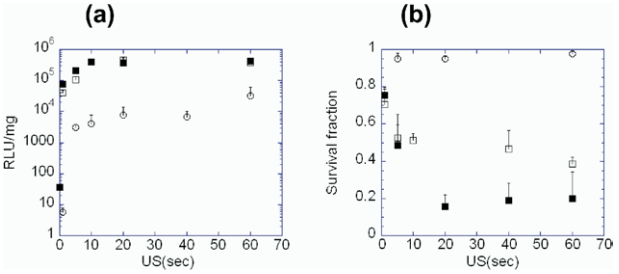


Fig. 6. Effect of the ultrasound exposure time on the luciferase activity and cell viability of CHO-E cells at a height of $H = 1$ mm. (a) Luciferase activity, (b) survival fractions measured by the MTT assay. Acoustic intensity, $I_A$, was 1.9 W/cm$^2$. The UCA concentration was 0% (open circle), 5% (open square), 20% (filled square) (vol/vol). The concentration of plasmid pGL3-control was 20 $\mu$g/mL.

This energy distribution has significant effects on the detachment and transfection of cells as the medium height decreases, *i.e.*, the intensity of the superposed ultrasonic waves and the interaction of cavitation bubbles with cells become dominant as the medium height decreases.

Since transfection efficacy increased with a decrease in medium height (see Fig. 3), we next investigated the effect of UCA concentrations (0.1 to 40% vol/vol, *i.e.*, $6.5 \times 10^5 - 2.6 \times 10^7$ microbubbles/mL) on gene expression and survival fraction at $H = 1$ mm, where cytotoxicity due to ultrasound alone was minimal (see Fig. 2). The exposure time $T_A$ was 20 s, while acoustic intensities were $I_A = 1.3$ W/cm$^2$ (filled triangle) and $I_A = 1.9$ W/cm$^2$ (filled circle), respectively. Addition of 0.1% of UCAs induced gene expression of $1.1 \times 10^5 \pm 2.9 \times 10^4$ RLU/mg for $I_A = 1.9$ W/cm$^2$ and $1.4 \times 10^4 \pm 3.3 \times 10^3$ RLU/mg for $I_A = 1.3$ W/cm$^2$ (Fig. 5a). Survival fraction was $0.77 \pm 0.01$ and $1.00 \pm 0.03$ (Fig. 5b), respectively. A maximal gene expression was obtained at 5% of UCAs and the expression became constant over the UCA concentration range 5% to 40 % (vol/vol). Since the spatial distribution of the ultrasound energy was formed in a Gaussian distribution, cells located in the central area were detached by the interaction of superposed ultrasound and cavitation bubbles as the height of medium decrease and the concentration of UCAs increases. Accordingly, the constant gene expression over the 5% to 40% can be attributed to cells located at the perimeter of the well (see Fig. 4).

We next investigated the level of gene expression as a function of ultrasound exposure times (0 to 60 s), with $H = 1$ mm (Fig. 6). The UCA concentrations used were 0% (open circle), 5% (open square) and 20% (filled square). There was a marked increase in gene expression for both UCA concentrations as ultrasound irradiation times increased between 0 and 10 s and became constant around 20 s. In contrast, cell survival fraction decreases with increasing ultrasound exposure, in the presence of UCAs, up to 20 s and thereafter plateaus.

From these results, it will be apparent that Optison™, an albumin based UCA, increases the efficacy of gene transfection into CHO-E cells *in vitro*, especially in the range of 1 to 2 mm height as seen Fig. 3. Next, we examined the hypothesis that similar efficacies could be obtained with albumin alone. We transfected cells with heat-treated crushed Optison™ solution (Fig. 7). The concentration of dissolved albumin UCA shell components in the transfection media were 5% (vol/vol) (open triangle) and 20% (vol/vol) (filled triangle). Luciferase activity increased with increasing ultrasound irradiation times. Maximal luciferase activity was recorded at 60 s, $3.8 \times 10^4 \pm 3.9 \times 10^3$ RLU/mg for 5% and $1.4 \times 10^5 \pm 1.8 \times 10^4$ RLU/mg for 20%, respectively. Interestingly, these values are almost the same as those obtained with transfection with ultrasound alone (see Fig. 5a). Similarly, the survival fraction is almost the same as that of ultrasound alone. The difference becomes evident at

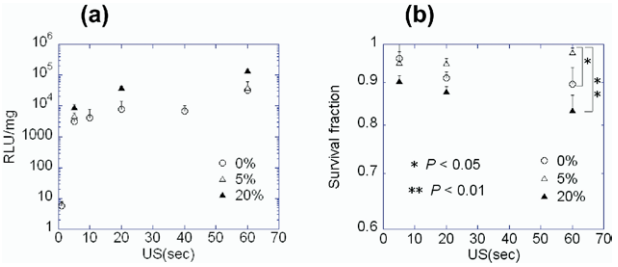


Fig. 7. Effect of the crushed heated Optison™ solution on the luciferase activity and cell viability of CHO-E cells at a height of $H = 1$ mm. (a) Luciferase activity, (b) survival fractions measured by the MTT assay. Acoustic intensity, $I_A$, was 1.9 W/cm$^2$. The solution concentration was 5% (open triangle) and 20% (filled triangle) (vol/vol). The concentration of plasmid pGL3-control was 20 $\mu$g/mL.

60 s, where the survival fraction is 0.90 ± 0.04 for 5% ($p < 0.05$ versus ultrasound alone) and 0.83 ± 0.04 for 20% ($p < 0.01$ versus ultrasound alone), respectively. The phenomena of capillary waves and subsequent atomized particles were hardly ever observed in these experiments.

## DISCUSSION

In this study, we have demonstrated gene transfection into CHO-E cells can be enhanced by low concentrations of UCAs using superposed ultrasound. When ultrasound is generated in a fixed position, standing waves are generated. Two types of nodes and antinodes are formed in the standing waves. Nodes of displacement occur at the same place as antinodes of pressure. Conversely, at the nodes of pressure, antinodes of displacement are generated.

We first investigated the effect of ultrasound alone on cell viability at a height of 1 mm when cells were located near the first node (displacement node) of the incident ultrasound downstream (Fig. 2). Ultrasound did not induce cells damage at the intensities of $I_A$ = 1.3 W/cm$^2$ and $I_A$ = 1.9 W/cm$^2$ up to exposure time of 120 s. This result correlates with the results of Pickworth et al. (Pickworth et al. 1989) that cells were not damaged at a node of displacement by 1.09 MHz continuous ultrasound of either 1W/cm$^2$ or 2W/cm$^2$, compared with cells at an antinode.

When UCAs are added, survival fraction was reduced by cavitation effects (Fig. 3). The transfection efficacy and survival fraction show opposite trends in the medium height (wave traveling distance), concentration of UCAs and exposure times of superposed ultrasound, *i.e.*, enhancement of transfection induces cytotoxicity. This tendency corresponds with previous experimental studies (Bao et al. 1997; Miller and Quddus 2001). As the medium height decreases, the intensity of superposed ultrasound and cavitation bubbles increases, resulting in cell detachment at the central area of 24-wells and in transfected cells at edge of the wells (Fig. 4). This detachment corresponds with a Gaussian model for the patterns of ultrasound energy. Also, stagnation of flow at the edge of the well bottom may enhance transduction. Although many studies have been performed with suspensions of cultured cells *in vitro* (Bao et al. 1997; Brayman and Miller 1997; Ogawa et al. 2002; Tata et al. 1997; Wang et al. 2005; Zarnitsyn and Prausnitz 2004), the effect of differences in transfection efficacy and survival fraction has not been previously described. At a height of 1 mm, just a 0.1% concentration of UCAs (*i.e.*, $6.5 \times 10^5$ microbubbles/mL) could induce high transfection with a high survival fraction. The results above indicate that cells located at nodes of motion do not depend on the pressure fluctuation but on the dynamic properties of cavitation bubbles.

Table 2. Characteristic of a $C_3F_8$ cavitation bubble

| | | | | |
|---|---|---|---|---|
| $P_A$ (MPa) | 0.19 | 0.23 | 0.26 | 0.28 |
| $P_{max}$ (MPa) | 855 | 5043 | 8950 | 10521 |
| $R_{min}$ (nm) | 79 | 45 | 38 | 36 |
| $R_{max}$ ($\mu$m) | 2.8 | 3.7 | 4.3 | 4.8 |

Positive pressure, $P_A$, measured by a PVDF needle hydrophone. The maximum pressure at the bubble rebound $P_{max}$, maximum bubble radius $R_{max}$, minimum bubble radius $R_{min}$, and were calculated from eqs 2, 3 and 4 using the fourth order Runge-Kutta method, where $R_0$ = 1 $\mu$m.

We hypothesized that complicated superposed ultrasound could enhance growth and collapse of cavitation bubbles created by collapse of UCAs, resulting in cell membrane damage and subsequent molecular delivery into cells. We shall attempt to define the cavitation bubble significantly involved. Assume that cavitation bubbles are generated from cavitation nuclei, proposed by the Harvey model (Harvey et al. 1944). This model is based on an assumption that gas is trapped within a crevice and a cavitation bubble is generated from the crevice due to the decrease in pressure. Suppose that the gas of Optison$^{TM}$, $C_3F_8$, is trapped within crevices of the debris produced by collapse of Optison$^{TM}$, and cavitation bubbles are generated from the crevices and behave as shown in eqn (2). The pressure at the bubble wall is given by eqn (3). The calculation was conducted for 50 $\mu$s using the fourth order Runge-Kutta method. Table 2 shows the maximum pressure at the bubble wall $P_{max}$, the minimum bubble radius $R_{min}$ and the maximum bubble expansion radius $R_{max}$ for different ultrasound pressures $P_A$, where the initial bubble radius $R_0$ was 1 $\mu$m. As $P_A$ increases, $P_{max}$ and $R_{max}$ increase, while $R_{min}$ decreases. For $P_A$ is 0.28 MPa, $P_{max}$ is 10521MPa, $R_{max}$ 4.8 $\mu$m and $R_{min}$ 0.036 $\mu$m. The theory was derived from an assumption that a cavitation bubble remains spherically symmetric, and both the liquid jet formation (Kodama and Tomita 2000; Tomita and Kodama 2003) and Taylor instability (Neppiras 1980) are ignored. Therefore, these values would be reduced by fission of collapsing bubbles (Brennen 2002) in the real flow field.

At every bubble rebound, high pressure is generated at the bubble wall, and resulting shock waves propagate outward. Let us suppose that shock waves interact with surrounding cells and subsequent cell membrane damage is thereby induced.

Now we estimate that the damage potential radius, $r_C$, by a single shock wave from the center of a cavitation bubble, as given by eqn (5) (Sundaram et al. 2003). Figure 8 shows the relationship between the potential radius for causing the membrane damage by the shock wave and bubble expansion for varying ultrasound pres-

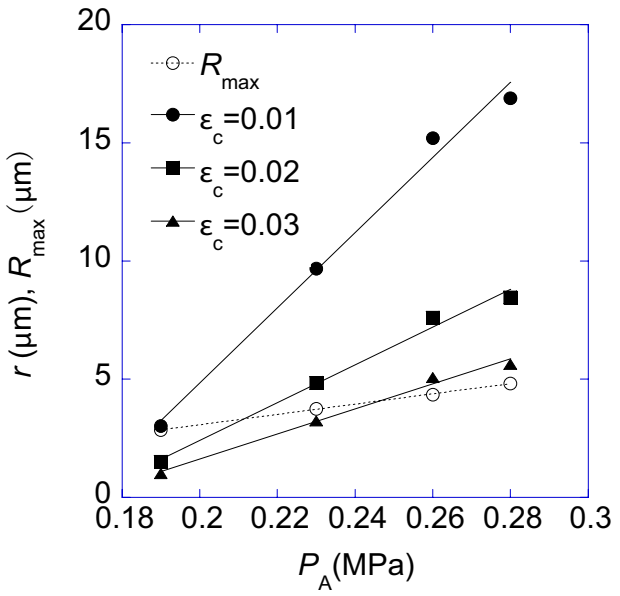


Fig. 8. Potential radius of inducing cell damage by a shock wave from a cavitation bubble, and the maximum bubble expansion radius, $R_{max}$. Ultrasound pressure, $P_A$ was varied from 0.19 MPa to 0.28 MPa. $\epsilon_C$ is the area strain of a cell membrane exposed to the shock wave, where $R_0 = 1$ $\mu$m. Numerical data were obtained using the fourth order Runge-Kutta method.

sures. The results suggest that the cell membrane will be damaged by the interaction of the shock wave when cells are located at more than 5 $\mu$m away from the center of the bubble. The pressure of the shock wave inversely decreases with increasing propagation distance, as given by eqn (6). Therefore, the transient membrane permeability will be induced between 5 $\mu$m and a certain distance from the center of the bubble in which exogenous molecules may be delivered into the cytoplasm. The cell membrane was found to be the most sensitive to the characteristic of shock waves propagating through the cell components (Steinbach et al. 1992). Because each cell line may show differences in intracellular densities and fluidities of membranes, the value of the shock wave-induced surface velocity may be different for each cell line, leading to different membrane permeability. Kodama et al. (2000) have reported that the impulse (defined as the integration of pressure with respect to time) of the shock wave might be an important factor governing the temporary permeability increase necessary for delivering macromolecules into cells. More recently, Koshiyama et al. (2004) performed molecular dynamics simulation of the interaction of a single shock wave with lipid bilayers and obtained the results that the impulse of the shock wave might increase, not only the penetration of endogenous molecules into the bilayers, but also the disorder of the alkyl chain and the fluidity of the lipid, which might be related to transient membrane permeability.

Molecular delivery using UCAs can transfer drug or genes to the specific sites within the target organ by disrupting UCAs circulating in the intravascular space (Bekeredjian et al. 2003). In the present study, it was shown that superposed ultrasound was able to enhance transfection ratio due to cavitation bubbles at a low concentration of UCAs. By devising a method to generate an optimized phase superposition of ultrasound in the body, we may improve efficacy of molecular delivery into target sites.

*Acknowledgments*—This study was supported by a grant from the UK Medical Research Council to MJKB (G0100120). TK acknowledges funding support from Special Coordination Funds for Promoting Science and Technology (MEXT), Grant-in-Aid for Specially Promoted Research (B), JSPS (17300168) and Grant-in-Aid for Scientific Research on Priority Area, MEXT (17012002). Y T acknowledges founding support from Short-Term Research Experience Fellowships in 2003 (MEXT). Optison™ was donated by Amersham Health Plc, Oslo, Norway.

## REFERENCES

Abbott JG. Rationale and derivation of MI and TI–a review. Ultrasound Med Biol 1999;25:431–441.

Aplin AE, Hogan BP, Tomeu J, Juliano RL. Cell adhesion differentially regulates the nucleocytoplasmic distribution of active MAP kinases. J Cell Sci 2002;115:2781–2790.

Bao S, Thrall BD, Miller DL. Transfection of a reporter plasmid into cultured cells by sonoporation *in vitro*. Ultrasound Med Biol 1997; 23:953–959.

Bekeredjian R, Chen S, Frenkel PA, Grayburn PA, Shohet RV. Ultrasound-targeted microbubble destruction can repeatedly direct highly specific plasmid expression to the heart. Circulation 2003; 108:1022–1026.

Brayman AA, Miller MW. Acoustic cavitation nuclei survive the apparent ultrasonic destruction of Albunex microspheres. Ultrasound Med Biol 1997;23:793–796.

Brennen C. Fission of collapsing cavitation bubbles. J Fluid Mech 2002;472:153–166.

Carstens CP, Kramer A, Fahl WE. Adhesion-dependent control of cyclin E/cdk2 activity and cell cycle progression in normal cells but not in Ha-ras transformed NRK cells. Exp Cell Res 1996;229:86–92.

Chen WS, Lu X, Liu Y, Zhong P. The effect of surface agitation on ultrasound-mediated gene transfer in vitro. J Acoust Soc Am 2004; 116:2440–2450.

Cheng T, Xu CY, Wang YB, et al. A rapid and efficient method to express target genes in mammalian cells by baculovirus. World J Gastroenterol 2004;10:1612–1618.

Chiba C. Study on atomization of liquid due to ultrasound oscillation. (PhD thesis) Engineering. Sendai: Tohoku University; 1983.

Danialou G, Comtois AS, Dudley RW, et al Ultrasound increases plasmid-mediated gene transfer to dystrophic muscles without collateral damage. Mol Ther 2002;6:687–693.

Dannenberg A, Suga M. Histochemical stain for macrophages. New York: Academic Press, 1981.

Dokka S, Rojanasakul Y. Novel non-endocytic delivery of antisense oligonucleotides. Adv Drug Deliv Rev 2000;44:35–49.

Evans EA, Waugh R, Melnik L. Elastic area compressibility modulus of red cell membrane. Biophys J 1976;16:585–595.

Everbach EC, Makin IR, Azadniv M, Meltzer RS. Correlation of ultrasound-induced hemolysis with cavitation detector output *in vitro*. Ultrasound Med Biol 1997;23:619–624.

Feril LB, Jr., Kondo T, Zhao QL, et al. Enhancement of ultrasound-induced apoptosis and cell lysis by echo-contrast agents. Ultrasound Med Biol 2003;29:331–337.
Fowlkes JB, Holland CK. Mechanical bioeffects from diagnostic ultrasound: AIUM concensus statements. (American Institute of Ultrasound in Medicine). J. Ultrasound Med 2000;19:69–72.
Greenleaf WJ, Bolander ME, Sarkar G, Goldring MB, Greenleaf JF. Artificial cavitation nuclei significantly enhance acoustically induced cell transfection. Ultrasound Med Biol 1998;24:587–595.
Harvey EN, Barnes DK, McElroy WD, Whiteley AH, Pease DC, Cooper KW. Bubble formation in animals. J Cell Comp Physiol 1944;24:1–22.
Kamaev PP, Hutcheson JD, Wilson ML, Prausnitz MR. Quantification of optison bubble size and lifetime during sonication dominant role of secondary cavitation bubbles causing acoustic bioeffects. J Acoust Soc Am 2004;115:1818–825.
Keller JB, Miksis M. Bubble oscillations of large amplitude. J Acoust Soc Am 1980;68:628–633.
Kodama T, Doukas AG, Hamblin MR. Delivery of ribosome-inactivating protein toxin into cancer cells with shock waves. Cancer Lett 2003;189:69–75.
Kodama T, Hamblin MR, Doukas AG. Cytoplasmic molecular delivery with shock waves: Importance of impulse. Biophys J 2000;79:1821–1832.
Kodama T, Tan PH, Offiah I, et al. Delivery of oligodeoxynucleotides into human saphenous veins and the adjunct effect of ultrasound and microbubbles. Ultrasound Med Biol 2005;31:1683–1691.
Kodama T, Tomita Y. Cavitation bubble behavior and bubble-shock wave interaction near a gelatin surface as a study of *in vivo* bubble dynamics. Appl Phys B-Lasers 2000;70:139–149.
Koike H, Tomita N, Azuma H, et al. An efficient gene transfer method mediated by ultrasound and microbubbles into the kidney. J Gene Med 2005;7:108–116.
Koshiyama K, Kodama T, Yano T, Fujikawa S. Molecular dynamic simulation of cell permeabilization induced by shock wave impulse. In: Ikohagi T Proceedings of The Fourth International Symposium on Advanced Fluid Information and the First International Symposium on Transdisciplinary Fluid Integration AFI/TFI2004 Sendai, Japan 2004, 36–37.
Lawrie A, Brisken AF, Francis SE, Cumberland DC, Crossman DC, Newman CM. Microbubble-enhanced ultrasound for vascular gene delivery. Gene Ther 2000;7(23):2023–2027.
Lee AG. How lipids affect the activities of integral membrane proteins. Biochim Biophys Acta 2004;1666:62–87.
Li T, Tachibana K, Kuroki M. Gene transfer with echo-enhanced contrast agents: comparison between Albunex, Optison, and Levovist in mice—initial results. Radiology 2003;229:423–428.
Lindner JR. Microbubbles in medical imaging: Current applications and future directions. Nat Rev Drug Discov 2004;3:527–532.
Lu QL, Liang HD, Partridge T, Blomley MJ. Microbubble ultrasound improves the efficiency of gene transduction in skeletal muscle *in vivo* with reduced tissue damage. Gene Ther 2003;10:396–405.
Mehier-Humbert S, Guy RH. Physical methods for gene transfer: Improving the kinetics of gene delivery into cells. Adv Drug Deliv Rev 2005;57:733–753.
Miller DL, Quddus J. Lysis and sonoporation of epidermoid and phagocytic monolayer cells by diagnostic ultrasound activation of contrast agent gas bodies. Ultrasound Med Biol 2001;27:1107–1113.
Neppiras EA. Acoustic cavitation. Phys Rep 1980;61:159–251.
Ogawa R, Kondo T, Honda H, Zhao QL, Fukuda S, Riesz P. Effects of dissolved gases and an echo contrast agent on ultrasound mediated *in vitro* gene transfection. Ultrason Sonochem 2002;9:197–203.
Pickworth MJ, Dendy PP, Twentyman PR, Leighton TG. Studies of the cavitational effects of clinical ultrasound by sonoluminescence, 4. The effect of therapeutic ultrasound on cells in monolayer culture in a standing wave field. Phys Med Biol 1989;34:1553–1560.
Steinbach P, Hofstadter F, Nicolai H, Rossler W, Wieland W. *In vitro* investigations on cellular damage induced by high energy shock waves. Ultrasound Med Biol 1992;18:691–699.
Sundaram J, Mellein BR, Mitragotri S. An experimental and theoretical analysis of ultrasound-induced permeabilization of cell membranes. Biophysical J 2003;84:3087–3101.
Taniyama Y, Tachibana K, Hiraoka K, et al. Local delivery of plasmid DNA into rat carotid artery using ultrasound. Circulation 2002;105:1233–1229.
Tata DB, Dunn F, Tindall DJ. Selective clinical ultrasound signals mediate differential gene transfer and expression in two human prostate cancer cell lines: LnCap and PC-3. Biochem Biophys Res Commun 1997;234:64–67.
Tennant JR. Evaluation of the trypan blue technique for determination of cell viability. Transplantation 1964;2:685–694.
Tomita Y, Kodama T. Interaction of laser-induced cavitation bubbles with composite surfaces. J Applied Physics 2003;94:2809–2816.
Wang X, Liang HD, Dong B, Lu QL, Blomley MJ. Gene transfer with microbubble ultrasound and plasmid DNA into skeletal muscle of mice: Comparison between commercially available microbubble contrast agents. Radiology 2005;237:224–229.
Yang L, Shirakata Y, Tamai K, et al. Microbubble-enhanced ultrasound for gene transfer into living skin equivalents. J Dermatol Sci 2005;40:105–114.
Zarnitsyn VG, Prausnitz MR. Physical parameters influencing optimization of ultrasound-mediated DNA transfection. Ultrasound Med Biol 2004;30:527–538.

## APPENDIX

*Atomized liquid particles generated with ultrasound*

The mean diameter, $d$, of the liquid particles due to capillary waves generated by ultrasound is give as a semiempiric equation (Chiba 1983)

$$d \cong 1.9\left[\frac{\sigma_L}{\rho_L f^2}\right]^{\frac{1}{3}} \tag{1}$$

where the acoustic frequency $f$ is varied from 20 kHz to 3 MHz. For water at 25°C, the liquid density, $\rho_L$, has a value of 997.04 kg/m$^3$, $\sigma_L$ is the liquid surface tension of 71.96 mN/m. Hence, the mean diameter of the atomized particles is given a value of 7.9 $\mu$m for 1-MHz ultrasound.

*Dynamics of a free cavitation bubble in the presence of ultrasound*

The radial motion of a bubble with a radius $R$ in compressible and Newtonian liquid, a Keller-Miksis model (Keller and Miksis 1980), is given by

$$R\dot{R}\left(1-\frac{1}{C_L}\dot{R}\right)+\frac{3}{2}\dot{R}^2\left(1-\frac{1}{3C_L}\dot{R}\right)=\left(1+\frac{\dot{R}}{C_L}\right)\frac{1}{\rho_L}\left[P_{r=R}(t)-P_C\left(t+\frac{R}{C_L}\right)-P_\infty\right]+\frac{R}{\rho_L C_L}\frac{dP_{r=R}(t)}{dt}. \tag{2}$$

The pressure, $Pr = R$, at the bubble surface is given by

$$P_{r=R}(t)=\left(P_\infty+\frac{2\sigma_L}{R_0}\right)\left(\frac{R_0}{R}\right)^{3\gamma}-\frac{2\sigma_L}{R}-\frac{4\mu_L}{R}\dot{R}. \tag{3}$$

The oscillation pressure term $P_C$ is given as

$$P_C(t)=\left|P_A\right|\sin\omega t \tag{4}$$

where, $C_L$ is the sound velocity in liquid (1497.3 m/s), $P_\infty$ atmospheric pressure (101.3 kPa), $R_0$ initial bubble radius, $\gamma$ adiabatic exponent of a gas (1.07), $\mu_L$ liquid shear viscosity (0.890 mPa · s), $P_A$ peak positive pressure measured in the experiments, $\omega$ the circular frequency.

Consider that a spherical shock wave is generated at the bubble rebound. The shock wave interacts with surrounding cells, resulting in cell membrane disruption. The radius from the center of the bubble, $r_C$,

for generating the disruption of the cell membrane is given as (Sundaram et al. 2003)

$$r_C \approx \frac{P_{\max} R_{\min}}{\varepsilon_C \rho_L C_L^2} \tag{5}$$

where $P_{\max}$ is the maximum pressure at the rebound when the bubble obtains the minimum radius $R_{\min}$ and $\epsilon_C$ is the static critical strain necessary to irreversibly disrupt the membrane. $\epsilon_C$ is estimated to be 0.02 to 0.03 for the membrane of red blood cells (Evans et al. 1976).

Suppose the shock wave pressure $P$s, defined as the peak value of the shock wave pressure, decreases as approximately $1/r$ while it propagates outwards, the following relation is given

$$P_S = \frac{P_{\max} R_{\min}}{r} \tag{6}$$